Chimica Techno Acta
published by Ural Federal University
eISSN 2411-1414
chimicatechnoacta.ru

ARTICLE
2023, vol. 10(3), No. 202310314
DOI: 10.15826/chimtech.2023.10.3.14

Effect of sintering duration on structure and properties of Ni-Al metal-intermetallic composites produced by SPS

Tatiana Ogneva [a] *, Alexander Anisimov [b], Ruslan Kuzmin [a], Andrey Tyurin [a], Yulia Emurlaeva [a], Natalya Aleksandrova [a]

a: Department of Materials Science, Novosibirsk State Technical University, Novosibirsk 630073, Russia
b: Lavrent'ev Institute of Hydrodynamics, Novosibirsk 630090, Russia
***** Corresponding author: ogneva@corp.nstu.ru

This paper belongs to the RKFM'23 Special Issue: https://chem.conf.nstu.ru/.
Guest Editors: Prof. N. Uvarov and Prof. E. Aubakirov.

Abstract

The fabrication of Ni-Al based metal-intermetallic layered (MIL) composites is one of the actively developing directions in the production of materials for aircraft and space industries. Alternating hard intermetallic layers with ductile metal layers provides a unique combination of mechanical properties. In this study, metal-intermetallic layered composites consisting of Ni and nickel aluminides were fabricated using spark plasma sintering (SPS) of Ni and Al foils 100 and 25 μm in thickness, respectively. Samples sintered at 1100 °C for 0.5, 3, and 8 min were obtained. The purpose of this study was to fabricate Ni-Al MIL composites with increased strength properties using SPS technique and to investigate the effect of sintering duration on structure and properties. The structure of the samples sintered for 0.5 min consisted of Ni layers and intermetallic layers containing the sublayers with stoichiometric and Ni-rich B2 NiAl, $L1_0$ twinned martensite NiAl. The tensile strength of such composites was 485 MPa. The intermetallic layers in the sample sintered for 3 min have more Ni-rich NiAl, martensite NiAl, and Ni_3Al phases, which promoted to an increase in tensile strength to 575 MPa. The sample sintered for 8 min consisted of Ni and a solid solution of Al in Ni and showed the highest tensile strength, 610 MPa, due to solid solution hardening in the interlayers. The samples did not break when applying bending load, which is the evidence of the good reliability and durability of the composites.

Keywords

spark plasma sintering
structure
properties
nickel aluminide
laminated composites
XRD
EDX

Received: 17.09.23
Revised: 07.10.23
Accepted: 07.10.23
Available online: 12.10.23

Key findings

- Ni-Al based metal-intermetallic layered composites were fabricated using SPS.
- Sintering duration increased Ni concentration in the intermetallic layers.
- The intermetallic layers consisted of stoichiometric and Ni-rich B2 NiAl, $L1_0$ twinned martensite NiAl and Ni_3Al phases.
- The composite sintered for 8 min consisted of Ni and Ni(Al) solid solution layers.
- The increase in duration of sintering led to an increase in tensile strength.

1. Introduction

Metal-intermetallic layered (MIL) composites are high-demand materials possessing a combination of high plasticity of metal layers and high hardness of intermetallic layers [1–4]. Alternating of metal and intermetallic layers reduces the possibility of sudden damage and allows achieving a high level of reliability and durability of the material.

MIL composites based on Ni and Al are given an increased attention due to the favorable properties of nickel aluminides, in particular, high elastic modulus and microhardness, low density, and high heat resistance. Besides, nickel aluminides have high wear and oxidation resistance [5–8]. These features make Ni-Al-based MIL composites an attractive material for producing housing elements for gas turbine engines, large vessels and pipes operating under high pressure, heat-exchange elements in cryogenic, chemical and energy equipment. Also, Ni-Al based MIL composites can withstand explosive loadings and can be applied

as heat- and wear resistant coatings for constructional metals and alloys [9–12].

Most techniques of the fabrication of Ni-Al MIL composites are based on joining and heating of multilayered packages consisting of alternating Ni and Al foils. For instance, such composites are typically manufactured using diffusion welding [13], or cold-rolling [11, 14, 15], explosive welding [16–19] with the subsequent heat or pressure treatment, and reaction synthesis [11, 12, 20–24]. In this work, the spark plasma sintering (SPS) technique was chosen to obtain the samples. First, distinguishing features of this technique are local heating to high temperatures and an intensive mass flow on the surfaces of sintered components [25–28]. These processes contribute to the fast heating and sintering of components and provide evaporation of impurities from the sintering surfaces before sintering. Second, electric current evenly flows through the entire volume of sintered materials, which leads to uniform temperature distribution throughout the entire volume of the sample and allows the synthesis of homogeneous high-quality composites.

Since the SPS technique was developed much later in comparison with the above mentioned widely known methods, the formation of MIL composites by SPS is still underinvestigated and requires deeper research. The present study is a continuation of our previous research described in [29], which was devoted to the effect of temperature and pressure on the structure and properties of Ni-Al MIL composites produced by SPS. Structural investigations in [29] revealed the formation of Ni_2Al_3, Al-rich NiAl, stoichiometric NiAl, and Ni-rich NiAl intermetallic phases. In addition, a needle-like martensitic NiAl structure was formed in the intermetallic layers due to fast cooling when the pulse current was turned off. The composites showed good mechanical properties that were compared with the results obtained by Mizuch et al. [30] whose work also was devoted to SPS sintering of Ni-Al MIL composites.

To achieve better mechanical properties of the Ni-Al MIL composites than those described in [29], the composition of the intermetallic layers should contain more Ni-rich phases (Ni-rich NiAl, Ni_3Al); at the same time, the formation of quite brittle Ni_2Al_3 phase should be avoided. Thus, in this study, the Ni/Al thickness ratio of the initial foils was increased to obtain more Ni-containing intermetallic phases. Besides, thinner Ni and Al foils were used for sintering to obtain smaller intermetallic grains.

It is known that when reducing the thickness of foils in a sintered Ni-Al package, the heat loss in the sample becomes less, the local temperature in reaction zone increases, therefore, less annealing time is needed to form intermetallic layers [8, 31]. Taking this into account, the annealing duration when sintering Ni and Al foils was reduced compared to the previous work [29]. Thus, the purpose of this research is to investigate the effect of sintering duration on the structure and properties of Ni-Al MIL composites produced by the SPS technique. Besides, the results are compared and analyzed with those obtained in our previous study, where thicker Ni and Al foils were used for sintering.

2. Materials and methods

2.1. Methods of investigation

Samples were produced at the Lavrentiev Institute of Hydrodynamics SB RAS on the Labox-1575 installation (Sinter Land Inc, Japan). Multilayer packages consisting of alternating 50 foils of Ni and 50 foils of Al with thicknesses of 100 and 25 μm, respectively, were used for sintering. Total thickness of the package gives a total thickness of the sample ~5 mm. Before sintering, the foils were cleaned in acetone bath for 20 min. The thickness of the initial plates was chosen such that after the reaction and diffusion processes between Ni and Al the laminated composite consisted of nickel aluminide layers and residual nickel. The sintering of multilayer packages was performed in graphite conductive molds consisting of a punch and a matrix. The internal diameter of the matrix was 30 mm. A graphite mold with multilayer packages was placed in the vacuum chamber. The pressure in the chamber during sintering was 10^{-2} Pa.

Three types of samples were obtained by SPS sintering. The variable parameter was an exposure time that was equal to 0.5, 3, and 8 min. During sintering, the samples were heated to 1100 °C at a heating rate of 50 °C/min, exposed at this temperature for 0.5, 3 and 8 min, and then cooled down to room temperature at a cooling rate of 350 °C/min. The temperature of sintering, 1100 °C, was chosen basing on the results of the previous study [29]. Lower temperature does not promote the formation of Ni-enriched intermetallic layers, higher temperature lead to extreme deformation of layers. The pressure applied to the pile during sintering with the punch was 30 MPa. The sintered materials were cylindrical samples with a diameter of 30 mm and a height of 5 mm.

2.2. Preparation of samples

Cutting of the samples for structural studies and mechanical tests was performed on a Sodick AG400L wire EDM machine. Specimens for metallography were prepared using standard techniques, including grinding and polishing. The samples were pressed into phenolic resin using a Buhler SimpliMet 1000 press. The surfaces of the samples were ground using abrasive paper of different grades (from 60 to 8 μm). Polishing was performed using an aqueous solution of aluminum oxide powder (particle size of 3 μm). At the final polishing stage, a colloidal solution of silica with a particle size of 0.04 μm was used. The structure of the Ni layers was revealed by chemical etching with concentrated nitric acid.

Metallographic studies were implemented using a semi-automatic microscope Axio Observer Z1m manufactured by Carl Zeiss. The images were recorded on an AxioCam MRc5 camera in the magnification range from ×50 to ×1600. Structural studies were performed in the bright field mode of the

 DOI: 10.15826/chimtech.2023.10.3.14

microscope. The grain structure of some intermetallic compounds was revealed in the differential interference contrast (DIC) mode. The elemental composition of the local zones of the samples was determined by energy-dispersive micro-X-ray spectral analysis using an INCA X-ACT analyzer (Oxfords Instruments) with a silicon-drift detector installed on a Carl Zeiss EVO 50XVP scanning electron microscope; the beam energy was 20 keV. Also, the scanning electron microscopy method was used for fractographic studies of samples after mechanical tests. The Vickers microhardness of the laminated composites was measured using a Wolpert Group 402MVD tester. The measurements were implemented in the vertical cross-section of the samples. The load on the diamond indenter was 0.098 N.

The fine structure of the samples was studied using a FEI Tecnai G2 20 TWIN transmission electron microscope (TEM) (maximum accelerating voltage 200 kV). The samples for TEM were prepared in the shape of round disks with a diameter of 3 mm, which were thinned on abrasive paper to a thickness of 80–100 μm. After that, a spherical hole was formed in the center of the samples on a Gatan Dimple Grinder Model 656 by grinding with abrasive pastes from 5 to 1 μm and polishing on an alumina suspension. Then, bombardment with argon ions was carried out on a Gatan PIPS equipment at an accelerating voltage of 5 kV until a hole in the center of samples with edges from 50 to 100 nm thick appeared.

The ARL X`TRA θ-θ diffractometer and the Petra III synchrotron radiation source (the German electron synchrotron / Deutsches Elektronen-Synchrotron – DESY) based at the German Helmholtz-Zentrum Geesthacht research center were used to determine the phase composition of the samples. X-ray diffraction patterns in both experiments were obtained from the cross-section of laminated samples. The source of radiation on the diffractometer was a copper X-ray tube with $K\alpha_1 + \alpha_2$ radiation. X-ray diffraction patterns were recorded in a discrete scanning mode with a step of 2θ = 0.05°; the dwell time was 5 s. At the synchrotron radiation source a Perkin Elmer XRD1621 2D detector with resolution 2048×2048 pixels was used. The radiation energy was 87.3 keV, the wavelength was 0.142 Å, and the contact spot size was 0.5×0.5 mm. The distance from the sample to the detector was 1795.5 mm.

To determine the strength properties under uniaxial tension conditions the tensile tests were performed on an Instron 3369 universal electromechanical testing machine. The moving speed of the crosshead was 0.5 mm/min.

3. Results and discussion

3.1. Structure of samples sintered with different holding duration

3.1.1. Structure of the sample sintered with the holding time of 0.5 min

X-ray diffraction results of the samples sintered for 0.5 min at 1100 °C are presented in Figure 1.

The XRD patterns of the laminated composite sintered for 0.5 min revealed that only Ni and intermetallic phases were present in the samples after sintering. No reflections of Al were found in the XRD patterns. As a result of the reaction between Ni and Al, all aluminum was consumed in the formation of intermetallic layers. As can be seen from the XRD patterns, the sample sintered for 0.5 min mainly consists of B2 NiAl intermetallic phase.

Metallographic images in the cross-section of the samples sintered for 0.5 min at 1100 °C are presented in Figure 2. The average thickness of intermetallic layers in this sample is about 18 μm. The thickness of Ni layers decreased from the initial 100 to 65 μm due to the plastic deformation under the applied pressure (Figure 2a). The sintering temperature was higher than the recrystallization temperature of Ni; therefore, the foils, which existed before sintering in the cold-rolled state, underwent recrystallization. The grain sizes are greater than the thickness of the Ni layer; a single Ni grain after sintering can reach the boundaries with intermetallic layers from both sides.

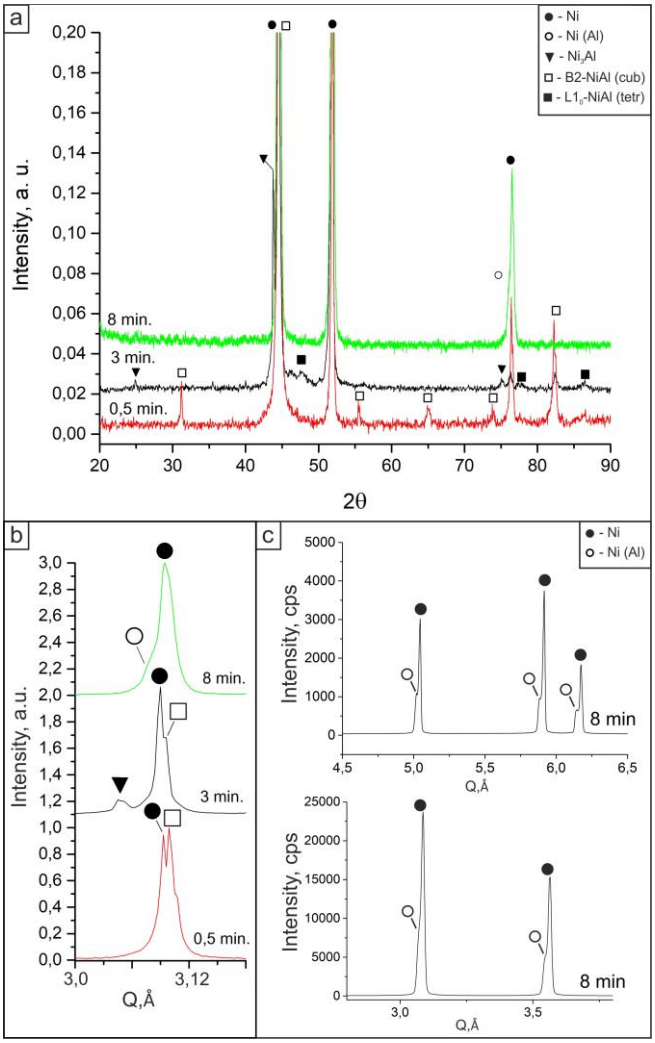

Figure 1 X-ray diffraction patterns of the Ni-Al MIL composites obtained by SPS for 0.5, 3, and 8 min: X-ray diffraction patterns recorded using diffractometer (a); X-ray diffraction patterns in Q of the peak corresponding to 2θ range ~38–47 degrees from the patterns in Figure 1a (b); X-ray diffraction patterns recorded using synchrotron facility (c).

 DOI: 10.15826/chimtech.2023.10.3.14

The twins appear in Ni grains after sintering, which is typical of the recrystallization process in fcc alloys (Figure 2a, inset).

The structure of the intermetallic layer consists of several sublayers (Figure 2b), the blue one in the middle and the light-brown ones on both sides of the middle sublayer. Besides, in the light-brown area adjoining the Ni layer, the needle-like layer becomes visible using DIC contrast. Point EDX analysis (Table 1 and Figure 2b) shows that the sublayer in the middle consists of 56.2–51.6 at.% of Ni and 43.8–48.4 at.% of Al, the light-brown sublayer contains 55.2–60.3 at.% of Ni and 39.7–44.8 at.% of Al, and the needle-like sublayer has 63.5–63.9 at.% of Ni and 36.1–36.5 at.% of Al. According to the Ni-Al phase diagram, all these regions belong to the NiAl intermetallic phase; however, the sublayer in the middle has a composition close to the equiatomic Ni/Al ratio, and the light-brown layer from the outside is enriched with Ni.

It is known that when the Ni concentration in a NiAl compound becomes more than 61.5 at.%, martensitic transformation occurs during rapid cooling of the alloy from temperatures over 1100 °C. Thus, in the sublayer containing 63.5–63.9 at.% of Ni, the martensitic needle-like structure forms in the intermetallic layer. NiAl martensite has a lamellar morphology, which is visible using DIC contrast in optical microscope. TEM image reveal that NiAl martensite in this sample consists of packages of microtwinned plates (Figure 3), the arrows in the figure indicate the twins.

The same fine structure of the martensite sublayer was observed in the previous work [29], where thicker Ni and Al foils were used for SPS sintering. NiAl martensite has a tetragonal crystal lattice with $L1_0$ structure. The fluorescence of Ni atoms in the Cu Kα radiation leads to the higher background of the X-ray pattern. Thus, the martensite reflections, which were present in a small amount, could not be visible in this case. Martensitic transformation occurs in former NiAl grains when cooling to 1100 °C. Thus, B2 NiAl zones and martensitic zones formed within the previous NiAl grains, as shown in Figure 3b (grain boundaries are indicated with arrows).

Note that the cooling rate fixed by the thermocouple during sintering was quite low for the martensitic transformation.

Table 1 Point EDX analysis results of the sample sintered for 0.5 min (points are shown in Figure 2b).

No. of point	Ni, at.%	Al, at.%
1	97.9	2.1
2	63.9	36.1
3	60.1	40.9
4	56.2	43.8
5	51.6	48.4
6	55.2	44.8
7	61.3	39.7
8	63.5	36.5
9	97.5	2.5

However, SPS technique allows achieving high heating and cooling rates in the local contact zones of the sintering materials. The process and the reasons for the NiAl martensitic transformation during SPS sintering were discussed in detail in the previous work [29], in which SPS sintering experiments with thicker foils at different temperature and pressure values were carried out.

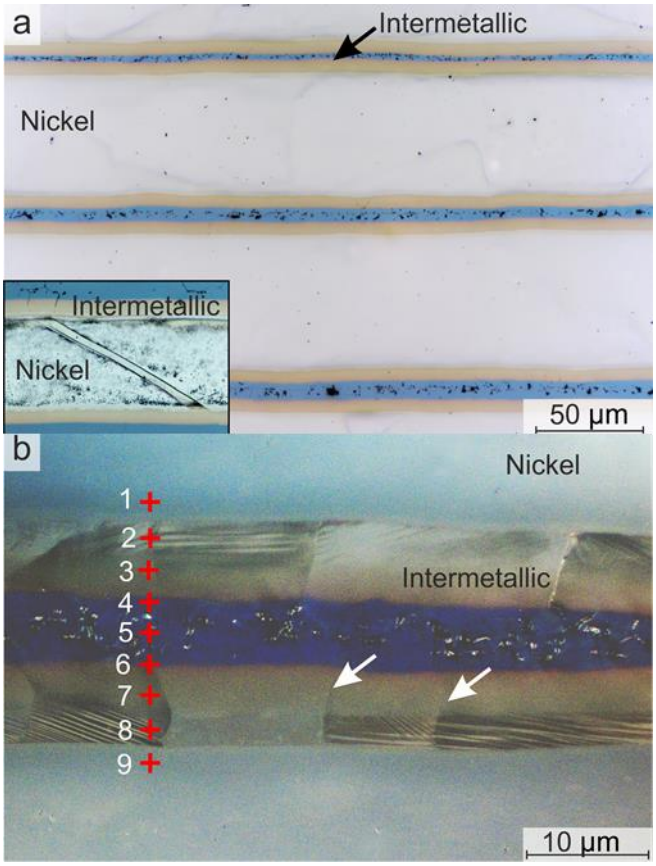

Figure 2 Structure of the Ni-Al MIL composites sintered by SPS for 0.5 min: overall cross-section view (BF mode) (a); the etched structure (inset); structure of the intermetallic layer in the cross-section (DIC mode) (b). The point numbers correspond to the numbers of the EDX spectra (Table 1).

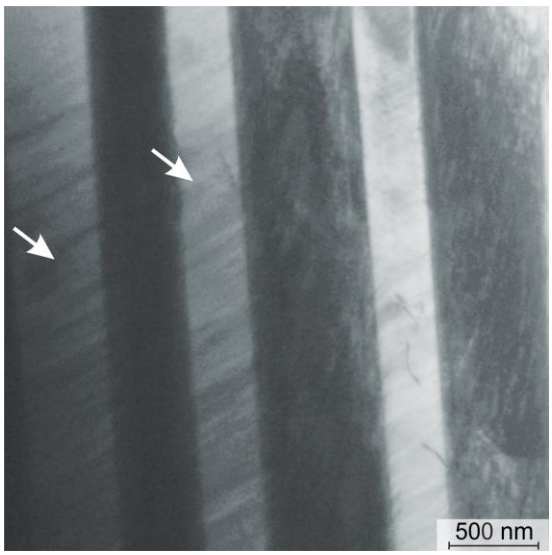

Figure 3 TEM image of the martensitic zone in the Ni-Al MIL composites sintered by SPS for 0.5 min.

 DOI: 10.15826/chimtech.2023.10.3.14

3.1.2. The structure of the sample sintered with the holding time of 3 min

The XRD pattern of the sample sintered for 3 min evidenced the formation of $L1_0$ NiAl and Ni_3Al intermetallic phases. The structure of the sample sintered for 3 min is shown in Figure 4. The average thickness of the intermetallic and Ni layers in this composite is similar to that of the sample sintered for 0.5 min and is 15 and 65 μm, respectively.

After etching, the sublayers of the identified phases are clearly visible in the intermetallic layer. Ni_3Al thin sublayer about several micrometers in thickness forms at the interface with nickel, where the concentration of Ni in intermetallic layer is the highest. Ni and Al contents in the Ni_3Al sublayer are 75 and 25 at.%, respectively (Table 2, Figure 4b). In the middle of the intermetallic layer, the concentration of Ni varies from 56.3 to 67.6 at.%, which is greater than that in the sample with a holding time of 0.5 min. Thus, the $L1_0$ NiAl martensite areas in this sample are larger, and the volume fraction of this phase is sufficient for detection using the XRD method.

When comparing the structure of the samples sintered for 0.5 and 3 min, it can be concluded that an increase in sintering time did not significantly influence the deformation rate of Ni layers compared with pressure and temperature parameters, as described in our previous study [29].

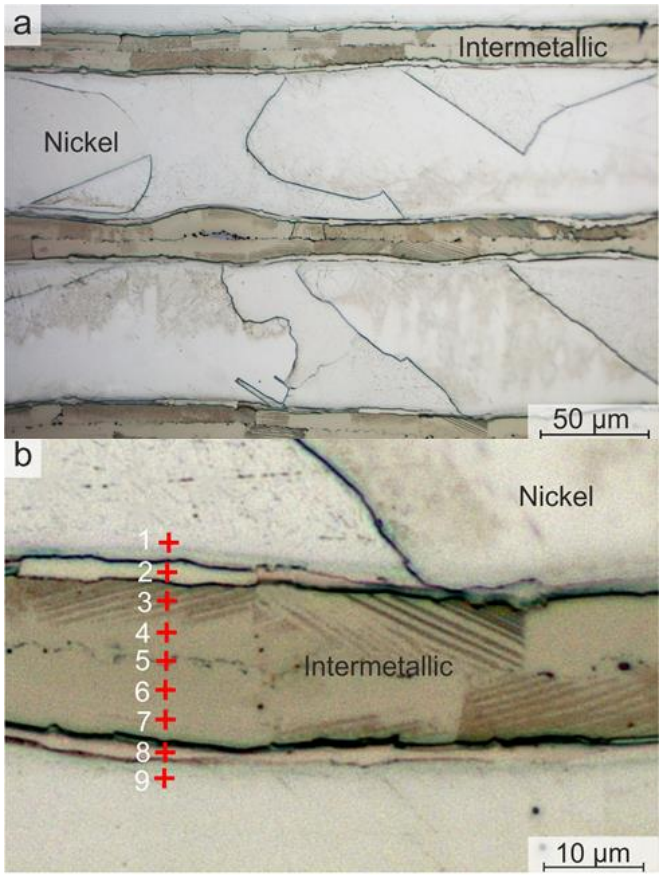

Figure 4 Etched structure of the Ni-Al MIL composites sintered by SPS for 3 min: overall cross-section view (a); structure of the intermetallic layer in the cross-section (b). The point numbers correspond to the numbers of the EDX spectra (Table 2).

A lot of experimental studies, for instance, [24, 31], have shown that an active exothermic reaction between Ni and Al starts after the complete melting of aluminum (660 °C). Further holding the sample at an elevated temperature promotes the diffusion of Ni and Al in the reaction layers. Thus, because of the increase in sintering duration, the thickness of the layers in the metal–intermetallic laminated composite was similar. However, using EDX analysis, it was determined that the increase in sintering duration led to greater saturation of intermetallic layers with Ni due to diffusion at high temperature. Thus, $L1_0$ NiAl and Ni_3Al phases with an increased concentration of Ni appeared in this sample.

3.1.3. The structure of the sample sintered 1100 °C with the holding time of 8 min

XRD investigation of the sample sintered for 8 min evidenced that no intermetallic phases formed after sintering. Only diffraction peaks of Ni were observed in the XRD patterns. More precise investigations of this sample were implemented by synchrotron X-ray diffraction. Synchrotron XRD patterns show the twinning of Ni peaks with the appearance of a “shoulder” on their left side that evidences the formation of a phase with crystal lattice parameters larger than those of pure Ni.

The layered structure of the sample and the results of its EDX analysis are shown in Figure 5 and Table 3. EDX analysis revealed that the sample consists of pure Ni layers and layers where the Al concentration gradually changes from 0 closer to Ni layers to 16–17 at.% closer to the middle of these layers.

The results of the SXRD and EDX analysis allow concluding that the sample sintered with a holding time of 8 min consists of Ni layers and layers of solid solution of Al in Ni. Since Al atoms have larger sizes than Ni atoms, the crystal lattice parameter of Ni(Al) solid solution is greater than that of pure Ni. Thus, the diffraction peaks of Ni(Al) solid solution shift to the left from the Ni peaks. The metallographic observations showed that the grain structure of Ni(Al) solid solution could not be revealed by etching with nitric acid. As previously described for all samples, the recrystallized grain sizes of Ni layers vary from 30 to 300 μm, and twinning also occurred during the process of recrystallization.

Table 2 Point EDX analysis results of the sample sintered for 3 min (Specters are shown in Figures 4b, respectively).

No. of point specter	Ni, at. %	Al, at. %
1	100	0
2	69.9	25.1
3	67.6	32.4
4	59.3	40.7
5	56.3	43.7
6	59.1	41.8
7	63.8	36.2
8	75.0	25.0
9	92.1	7.9

DOI: 10.15826/chimtech.2023.10.3.14

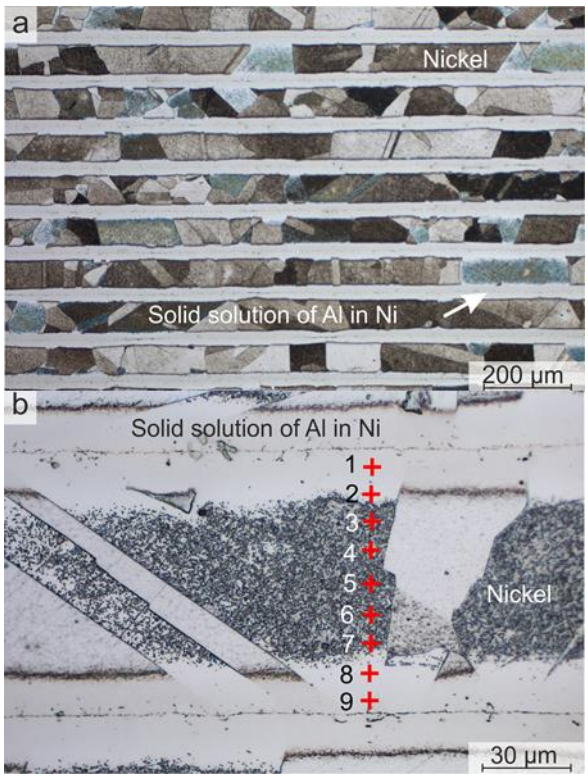

Figure 5 Structure of the Ni-Al MIL composites sintered by SPS for 8 min: (a) overall cross-section view; (b) structure of the intermetallic layer in the cross-section. The point numbers correspond to the numbers of the EDX spectra (Table 3).

Table 3 Point EDX analysis results of the samples (the points are shown in Figure 5b).

No. of point	Ni, at.%	Al, at.%
1	83.1	16.9
2	94.2	5.8
3	100	0
4	100	0
5	100	0
6	100	0
7	100	0
8	87.1	12.9
9	84.4	15.6

Besides, it can be clearly seen that the twins propagate through the Ni and Ni(Al) solid solution layers, indicating the absence of intergranular boundaries between Ni and Ni(Al) solid solution areas.

The average thickness of Ni(Al) solid solution layers is ~36 μm. Due to the fact that all Al dissolved in the Ni lattice after 8 min of holding at 1100 °C, the thickness of the solid solution layers is two times greater than that of the intermetallic layers in the abovementioned metal-intermetallic samples. Thus, the thickness of the Ni layers is slightly less than that in the samples described above and is equal to 60 μm.

Note that the concentration of Al in Ni(Al) solid solution exceeds the equilibrium one. This could be related to the high cooling rates in the local zones of the material. Probably, the local concentration inhomogeneities preventing the precipitation of nanosized intermetallic phases could appear under similar conditions. For instance, in [23] Ni_3Al nanoprecipitations appeared in Ni_3Al were observed in the Ni layer of the multilayered Ni-Al MIL composite after annealing for 1 h at 1100 and 1200 °C.

3.2. Mechanical properties of the samples

3.2.1. Microhardness of the samples

The thickness of the intermetallic layers is quite small; therefore, it was possible to measure only the average Vickers microhardness values of the entire intermetallic layer. The average value of microhardness in the samples sintered with a holding time 0.5 min is 3520 MPa, and in the samples sintered for 3 min – 3100 MPa. The microhardness level of the intermetallic layers is related to the Ni/Al ratio in the NiAl composition and varies from ~2380 to 4500 MPa. The deviations in the equiatomic composition led to an increase in NiAl microhardness [7]. This increase is explained by the lattice distortion caused by the greater dislocation density of the non-stoichiometric NiAl composition. The avarage microhardness of intermetallic layers containing mostly from Ni-rich NiAl corresponds to the literature data. The average microhardness of NiAl martensite is less than that of NiAl; thus, the intermetallic layers in the sample sintered for 3 min are slightly less hard than those sintered for 0.5 min.

The microhardness of the solid solution sublayers in the sample sintered for 8 min varies from 1750 MPa in the middle of the sublayer to 1650 MPa near the interface with Ni. The increased microhardness in the center is due to the increased concentration of Al atoms in the Ni crystal lattice. Dissolved Al atoms promote a higher dislocation density and solid solution strengthening.

Ni foils before sintering were in the cold-rolled state, and the microhardness of the Ni foils in the cross-section was 2000 MPa. After sintering for 0.5 and 3 min, the microhardness of the Ni layers in the samples decreased to 1120 MPa. After sintering for 8 min, the microhardness of the Ni layers decreased to 1000 MPa. Probably because of the longer holding time, the recrystallization process is more complete in this case.

3.2.2. Tensile test results of the samples

A diagram of the tensile strength of the samples is presented in Figure 6. The tensile strength values for the samples sintered for 0.5 and 3 min are 485 and 575 MPa, respectively. The higher values for the sample sintered for 3 min can be explained by the fact that less hard nickel aluninides, as a rule, are less brittle and have higher strength.

The tensile strength of Ni is ~355 MPa. The volume fraction of the intermetallic phases in both samples is approximately 20% of the total material of the laminated composites. According to the mixture rule, this is an evidence of the relatively high strength of the intermetallic component in the composite. Its value is comparable to the strength properties of ultrafine intermetallics produced by advanced powder metallurgy sintering techniques.

 DOI: 10.15826/chimtech.2023.10.3.14

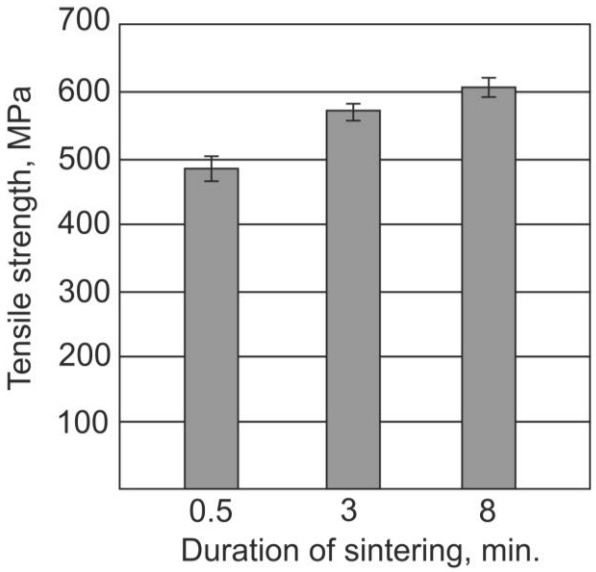

Figure 6 Tensile strength of the Ni-Al MIL composites sintered by SPS during 0.5, 3, and 8 min.

In addition, the stresses near the interfaces between the metal and intermetallic layers (or solid solution layers – in the case of 8 min of sintering) can positively affect the strength properties of the laminated composites.

The sample sintered with a holding time of 8 min exhibited the highest tensile strength of 610 MPa. The results can be explained as follows. First, the highest strength values of this sample are related to solid solution hardening. Also, the suggestion can be made that the local inhomogeneities of element concentration preventing the precipitation of nanoparticles of intermetallic phases could take place.

Second, as shown in Figures 2b, 4b, and 5b, Kirkendall porosity is observed in the middle of the intermetallic (samples 0.5 and 3 min) and solid solution (sample 8 min) layers, which is due to the different diffusion rates of Ni and Al atoms in the intermetallic layers. As can be seen in the microstructure images, with the increase in the holding time, the Kirkendall porosity noticeably decreases, which also contributes to the increase in the tensile strength.

Bending tests also were implemented in this study by analogy with our previous investigations in [29], where more thick Ni and Al foils were sintered. The bending tests were carried out with a load applied both parallel and perpendicular to the interfaces of the composites. In [29], some samples broke under the loading applied perpendicular to the layers of the composite, but some of them did not break when loading was applied parallel to the layers. However, the samples produced in this study remained unbroken during the testing in both ways. In addition, the macrostructure of the composite remained intact; no delamination was noticed in the bent samples. Thus, it can be concluded that the samples obtained in this work have higher reliability and can withstand bending load without breaking in spite of the presence of brittle intermetallic layers in the composite. Figure 7 illustrates the sample sintered for 0.5 min after the bending test when the force was applied perpendicular to the layers.

Figure 7 The sample sintered for 0.5 min bending tests when applying the force perpendicular to the layers.

3.2.3. Fracture morphology of the samples

The fracture surface after tensile tests of the samples sintered with the holding time of 0.5, 3 and 8 min at 1100 °C are presented in Figure 8 a–c, respectively. The morphology of the nickel layers after the tests indicates the ductile mechanism of fracture. Intermetallic layers due to their high hardness are characterized by brittle fracture surface.

In the sample sintered for 0.5 min, the layers of nickel and intermetallics delaminate from each other during the tensile test, and the interlayer cracks can be observed on the fracture surface (indicated with red arrows in Figure 8a). No delimitation occurs in the middle of the intermetallic layers, as was noticed in the samples sintered at the same SPS regimes with thicker Ni and Al plates in the previous study [29]. Stronger connection of the intermetallic half-layers is explained by lower Kirkendall porosity in the samples produced in this study, as described in the previous paragraph.

Similar fracture and delamination behavior are typical also for the sample sintered for 3 min (Figure 8b). However, in this sample, the interface between the intermetallic layer and Ni remains unbroken. In this sample, a thin Ni_3Al layer adjoining Ni was discovered. Ni_3Al has the same fcc lattice crystal type and the lattice parameter close to that of Ni, which provides stronger adhesion between nickel and the intermetallic layer.

In the sample sintered for 8 min, the nickel and Ni(Al) solid solution layers exhibited ductile fracture behavior over the entire fracture surface of the sample (Figure 8c). The Ni (Al) solid solution and Ni have the same fcc crystal lattices with very close parameters, and the zones of the Ni (Al) solid solution and Ni do not have boundary interfaces. Therefore, no delamination occurred between these layers. In addition, the solid solution sublayers did not delaminate in the middle due to practically no Kirkendall porosity.

4. Limitations

The remaining issue related to the present study is to investigate the fine structure in the Ni(Al) solid solution sublayers, which will allow understanding the principles of hardening in these areas, and to establish if there are any formation of Ni_3Al nanoprecipitations, typically observed in the samples fabricated by conventional methods.

 DOI: 10.15826/chimtech.2023.10.3.14

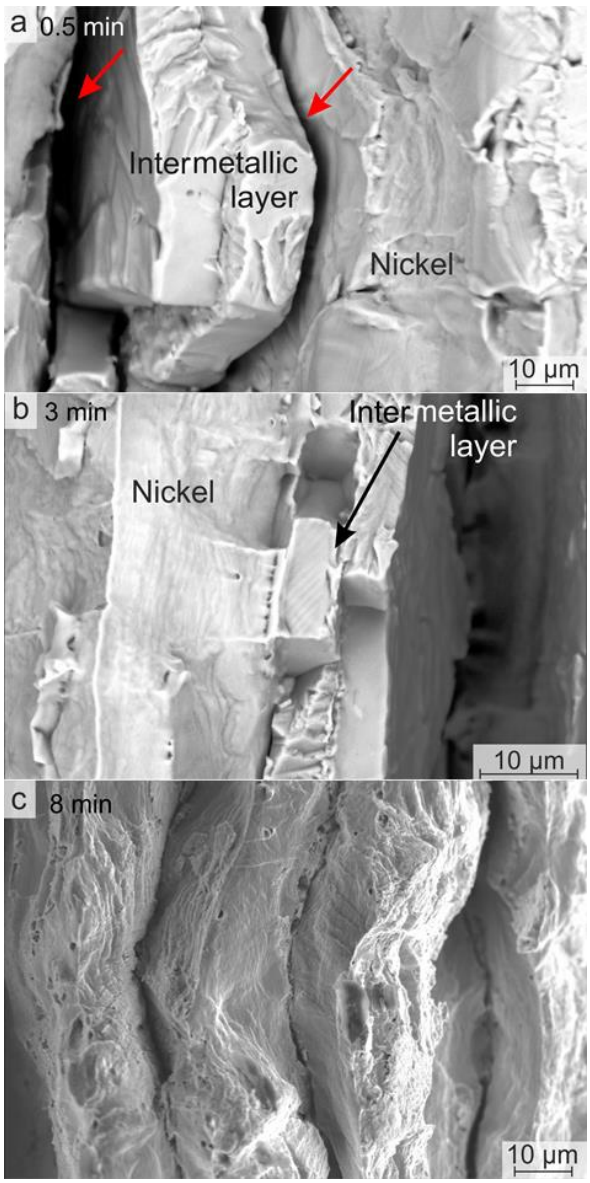

Figure 8 Fracture surface the Ni-Al MIL composites sintered by SPS for 0.5 (a), 3 (b), and 8 (c) min.

Of great interest in further research in the field of producing laminated composites is the formation and investigation of composites based on Ni and Ti alloys reinforced by intermetallic and ceramic components.

5. Conclusions

As a result of reaction between Ni and Al foils during SPS, the multilayered composites consisted of alteranating layers of ductile Ni and hard nickel aluminides were formed when sintering at 1100 °C at 0.5 and 3 min. Increasing the sintering duration from 0.5 to 3 min led to the formation of the intermetallic layers more saturated with Ni, such as NAl matrensite and Ni_3Al. Thus, greater Ni-enriched nickel aluminide phases were formed. In the case of sintering for 8 min Al atoms dissolved in nickel crystal lattice, and the samples after sintering consisted of Ni and Ni(Al) solid solution layers. Increasing the sintering duration led to an increase in the tensile strength of the samples due to the formation of more Ni-saturated intermetallic or Ni(Al) solid solution layers. The samples did not break when applying bending load, indicating high reliability and durability of the obtained MIL composites.

• Supplementary materials

No supplementary materials are available.

• Funding

This study was funded according to the Federal Task of Ministry of Science and Higher Education of the Russian Federation (project FSUN-2020-0014 (2019-0931): “Investigations of Metastable Structures Formed on Material Surfaces and Interfaces under Extreme External Impacts”.

• Acknowledgments

Structural research was conducted at NSTU Materials Research Center.

• Author contributions

Conceptualization: T.S.O.
Data curation: T.S.O.
Formal Analysis: T.S.O.
Funding acquisition: T.S.O.
Investigation: T.S.O., A.G.A., R.I.K., N.S.A., E.Yu.Yu., A.G.T.
Methodology: T.S.O., A.G.A., R.I.K., N.S.A., E.Yu.Yu., A.G.T.
Project administration: T.S.O.
Resources: T.S.O., A.G.A.
Software: T.S.O., R.I.K.
Supervision: T.S.O.
Validation: T.S.O., R.I.K.
Visualization: T.S.O.
Writing – original draft: T.S.O.
Writing – review & editing: T.S.O.

• Conflict of interest

The authors declare no conflict of interest.

• Additional information

Author IDs:
Tatiana Ogneva, Scopus ID 56905353300;
Alexander Anisimov, Scopus ID 7102276264;
Ruslan Kuzmin, Scopus ID 57189894268;
Andrey Tyurin, Scopus ID 25032105200;
Yulia Emurlaeva, Scopus ID 57205199327;
Natalya Aleksandrova, Scopus ID 57216883212.

Websites:
Novosibirsk State Technical University, https://en.nstu.ru/;
Lavrent’ev Institute of Hydrodynamics, http://www.hydro.nsc.ru/.

 DOI: 10.15826/chimtech.2023.10.3.14

References

1. Denisov I, Shakhray D, Malakhov A, Seropyan S. Combustion synthesis of metal-intermetallic-ceramic laminate AlMg6-NiAl-TiC composite. Crystals. 2022;12(12). doi:10.3390/cryst12121851
2. Bogdanov AI, Kulevich VP, Shmorgun VG. Microstructure evolution and growth of interfacial intermetallic compounds in NiCr/Ti alloy laminated composite after explosive welding and heat treatment. Metals (Basel). 2023;13(8). doi:10.3390/met13081417
3. Ye Q, Li X, Tayyebi M, Assari AH, Polkowska A, Lech S, Polkowski W, Tayebi M. Effect of heat treatment parameters on microstructure evolution, tensile strength, wear resistance, and fracture behavior of Ni–Ti multilayered composites produced by cross-accumulative roll bonding. Arch Civ Mech Eng. 2022;23(1):27. doi:10.1007/s43452-022-00557-8
4. Seropyan S, Saikov I, Andreev D, Saikova G, Alymov M. Reactive Ni–Al-based materials: strength and combustion behavior. Metals (Basel). 2021;11(6). doi:10.3390/met11060949
5. Malakhov A, Shakhray D, Denisov I, Galiev F, Seropyan S. Synthesis of NiAl intermetallic compound under shock-wave extrusion. Mater (Basel). 2022;15(17). doi:10.3390/ma15176062
6. Shevtsova L, Mali V, Bataev A, Anisimov A, Dudina D. Microstructure and mechanical properties of materials obtained by spark plasma sintering of Ni3Al–Ni powder mixtures. Mater Sci Eng A. 2020;773:138882. doi:10.1016/j.msea.2019.138882
7. Miracle DBB. The physical and mechanical properties of NiAl. Acta Metall Mater. 1993;41(3):649–684. doi:10.1016/0956-7151(93)90001-9
8. Simões S, Viana F, Ramos AS, Vieira MT, Vieira MF. Anisothermal solid-state reactions of Ni/Al nanometric multilayers. Intermetal. 2011;19(3):350–356. doi:10.1016/J.INTERMET.2010.10.021
9. Wang Y, Wang H, Liu X, Vecchio KS. Microstructure evolution in pure Ni and Invar-based Metallic-Intermetallic Laminate (MIL) composites. Mater Sci Eng A. 2017;682:454–465. doi:10.1016/j.msea.2016.11.033
10. Wang Y, Wang H, Liu X, Vecchio KS. Microstructure evolution in Ni and Ni-superalloy based metallic-intermetallic laminate (MIL) composites. Intermetal. 2017;87:70–80. doi:10.1016/j.intermet.2017.04.009
11. Srivastava VC, Singh T, Ghosh Chowdhury S, Jindal V. Microstructural characteristics of accumulative roll-bonded Ni-Al-based metal-intermetallic laminate composite. J Mater Eng Perform. 2012;21(9):1912–1918. doi:10.1007/s11665-011-0114-y
12. Konieczny M. Mechanical properties and deformation behavior of laminated Ni-(Ni2Al3+NiAl3) and Ni-(Ni3Al+NiAl) composites. Mater Sci Eng A. 2013;586:11–18. doi:10.1016/j.msea.2013.08.002
13. Kwiecien I, Bobrowski P, Wierzbicka-Miernik A, Litynska-Dobrzynska L, Wojewoda-Budka J. Growth Kinetics of the Selected Intermetallic Phases in Ni/Al/Ni System with various nickel substrate microstructure. Nanomater. 2019;9(2). doi:10.3390/nano9020134
14. Ji C, He Y, Wang CT, He Y, Pan X, Jiao J, Guo L. Investigation on shock-induced reaction characteristics of an Al/Ni composite processed via accumulative roll-bonding. Mater Des. 2017;116:591–598. doi:10.1016/j.matdes.2016.12.002
15. Battezzati L, Pappalepore P, Durbiano F, Gallino I. Solid state reactions in Al/Ni alternate foils induced by cold rolling and annealing. Acta Mater. 1999;47(6):1901–1914. doi:10.1016/S1359-6454(99)00040-3
16. Kwiecien I, Bobrowski P, Janusz-Skuza M, Wierzbicka-Miernik A, Tarasek A, Szulc Z, Wojewoda-Budka J. Interface characterization of Ni/Al bimetallic explosively welded plate manufactured with application of exceptionally high detonation speed. J Mater Eng Perform. 2020;29(10):6286–6294. doi:10.1007/s11665-020-05117-w
17. Kwiecien I, Wierzbicka-Miernik A, Szczerba M, Bobrowski P, Szulc Z, Wojewoda-Budka J. On the dsintegration of A1050/Ni201 explosively welded clads induced by long-term annealing. Mater (Basel). 2021;14(11). doi:10.3390/ma14112931
18. Bataev IA, Ogneva TS, Bataev AA, Mali VI, Esikov MA, Lazurenko D V, Guo Y, Jorge Junior AM. Explosively welded multilayer Ni–Al composites. Mater Des. 2015;88:1082–1087. doi:10.1016/j.matdes.2015.09.103
19. Guo X, Ma Y, Jin K, Wang H, Tao J, Fan M. Effect of stand-off distance on the microstructure and mechanical properties of Ni/Al/Ni laminates prepared by explosive bonding. J Mater Eng Perform. 2017;26(9):4235–4244. doi:10.1007/s11665-017-2890-5
20. Fan GH, Wang QW, Du Y, Geng L, Hu W, Zhang X, Huang YD. Producing laminated NiAl with bimodal distribution of grain size by solid–liquid reaction treatment. Mater Sci Eng A. 2014;590:318–322. doi:10.1016/j.msea.2013.10.038
21. Kim HY, Chung DS, Enoki M, Hong SH. Tensile and fracture properties of NiAl/Ni micro-laminated composites prepared by reaction synthesis. J Mater Res. 2006;21(5):1141–1149. doi:10.1557/jmr.2006.0154
22. Xia Z, Liu J, Zhu S, Zhao Y. Fabrication of laminated metal–intermetallic composites by interlayer in-situ reaction. J Mater Sci. 1999;34(15):3731–3735. doi:10.1023/A:1004624012683
23. Wang H, Han J, Du S, Northwood DO. Reaction synthesis of nickel/aluminide multilayer composites using Ni and Al foils: microstructures, tensile properties, and deformation behavior. Metall Mater Trans A. 2007;38(2):409–419. doi:10.1007/s11661-006-9066-5
24. Kim HY, Chung DS, Hong SH. Reaction synthesis and microstructures of NiAl/Ni micro-laminated composites. Mater Sci Eng A. 2005;396(1):376–384. doi:10.1016/j.msea.2005.01.044
25. Hulbert DM, Jiang D, Dudina D V, Mukherjee AK. The synthesis and consolidation of hard materials by spark plasma sintering. Int J Refract Met Hard Mater. 2009;27(2):367–375. doi:10.1016/j.ijrmhm.2008.09.011
26. Vidyuk TM, Dudina D V, Korchagin MA, Gavrilov AI, Skripkina TS, Ukhina A V, Anisimov AG, Bokhonov BB. Melting at the inter-particle contacts during Spark Plasma Sintering: Direct microstructural evidence and relation to particle morphology. Vacuum. 2020;181:109566. doi:10.1016/j.vacuum.2020.109566
27. Dudina D V, Kvashnin VI, Bokhonov BB, Legan MA, Novoselov AN, Bespalko YN, Jorge AM, Koga GY, Ukhina A V, Shtertser AA, Anisimov AG, Georgarakis K. Metallic iron or a Fe-based glassy alloy to reinforce aluminum: reactions at the interface during spark plasma sintering and mechanical properties of the composites. J Compos Sci. 2023;7(7). doi:10.3390/jcs7070302
28. Hu Z-Y, Zhang Z-H, Cheng X-W, Wang F-C, Zhang Y-F, Li S-L. A review of multi-physical fields induced phenomena and effects in spark plasma sintering: fundamentals and applications. Mater Des. 2020;191:108662. doi:10.1016/j.matdes.2020.108662
29. Ogneva TS, Bataev IA, Mali VI, Anisimov AG, Lazurenko D V, Popelyukh AI, Emurlaeva YY, Bataev AA, Tanaka S, Yegoshin KD. Effect of sintering pressure and temperature on structure and properties of NiAl metal-intermetallic composites produced by SPS. Mater Charact. 2021;180:111415. doi:10.1016/j.matchar.2021.111415
30. Mizuuchi K, Inoue K, Sugioka M, Itami M, Lee J, Kawahara M. Properties of Ni-aluminides-reinforced Ni-matrix laminates synthesized by pulsed-current hot pressing (PCHP). Mater Sci Eng A. 2006;428(1):169–174. doi:10.1016/j.msea.2006.04.113
31. Kim HY, Chung DS, Hong SH. Intermixing criteria for reaction synthesis of Ni/Al multilayered microfoils. Scr Mater. 2006;54(9):1715–1719. doi:10.1016/j.scriptamat.2005.12.032

 DOI: 10.15826/chimtech.2023.10.3.14